Indian J. Phys. **81 (10)** 1069-1077 (2007)

IJP

Selective interchannel coupling as computational strategy to interpret complex atomic spectrum

H R Varma, T Banerjee* and P C Deshmukh
Department of Physics, Indian Institute of Technology Madras, Chennai-600 036, India

E-mail : pcd@physics.iitm.ac.in

Abstract : Selective interchannel coupling has been used in the present work as an effective computational strategy to identify specific autoionization resonances and other correlation effects in the photoionization angular distribution asymmetry parameter for the case of valence *ns* subshell photoionization of atomic krypton and mercury. It is found that in the case of 6s photoionization of Hg, deviation of β from the non-relativistic value 2 in the energy region below the 5*d* ionization thresholds is a cumulative effect of the Cooper minimum in 6*s* photoionization and resonant excitations from the 5*d* subshells.

Keywords : autoionization resonances, relativistic random phase approximations, relativistic multichannel quantum defect theory

PACS No. : 32.80.Dz

1. Introduction

Autoionization is a many-body phenomenon in the photoabsorption process that occurs as a result of the interference between the degenerate ionization and excitation channels [1]. It causes significant fluctuations in the photoionization parameters. Understanding the process of autoionization is very crucial to extract information about the atomic spectrum and it can provide a great deal of information about relativistic and many-body effects. In addition, study of autoionization phenomena provides a good understanding of several related processes such as dielectronic recombination, stellar and tokamak plasma processes *etc.* Autoionization studies are also important to get information about metastable states that may have specific application in the production of lasers [2].

Atomic spectrum in the region of autoionization is extremely complex. Identification of resonances is a tedious work. Theoretical techniques come handy in this regard

*Corresponding Author
Present address : Department of Physics,
Manipal Institute of Technology, Manipal-576 104, Karnataka, India

since they enable selective treatment of the final state correlations. Relativistic Random Phase approximation (RRPA) is one such powerful many-body technique which include final state correlations through interchannel coupling [3]. The loss of gauge invariance of RRPA resulting from the exclusion of channels that are left out is rather minor [4] Thus, by making use of selective truncation of the RRPA, the atomic spectra can be characterized since channels that are excluded can only be associated with missing features in the computed spectrum. The Relativistic Multichannel Quantum Defect Theory (RMQDT) when used in conjunction with the RRPA, provides additional strength to the computational strategy [5]. The RMQDT allows one to characterize the dynamics of photoionization processes in terms of a few parameters, namely the eigen quantum defects μ_α, the eigen-dipole amplitudes D_α, and the transformation matrices $U_{k\alpha}$. The quantum defects parameters depend only on the short-range part of the potential and are nearly insensitive to energy. The RMQDT parameters are obtained from RRPA by doing calculations at a few energy points in the vicinity of the inner-shells which are closed for photoionization, and their insensitivity to energy enables interpolation in the autoionization energy region of interest.

In the present work is studied the photoionization angular distribution asymmetry parameter β for valence *ns* subshells of atomic krypton and mercury in the energy region of autoionization resonances generated by the interference of photoionization channels from *ns* subshell and excitation channels from $(n-1)d$ subshells. The relativistic expression of β is :

$$\beta_{ns} = \frac{\left|D_{1/2\to 3/2}\right|^2 + \sqrt{2}(D_{1/2\to 1/2}D^*_{1/2\to 3/2} + c.c)}{\left|D_{1/2\to 3/2}\right|^2 + \left|D_{1/2\to 3/2}\right|^2}. \tag{1}$$

In the non-relativistic limit β is independent of photon energy and takes a constant value $\beta = 2$. The deviation of β from its non-relativistic limit $\beta = 2$ occurs in the vicinity of Cooper minima, as the two relativistic amplitudes go through respective 'zero' at different energies [6]. At high photon energies, where *j*-dependent relativistic effects can become large, strong interchannel coupling [7,8] can cause significant differences in the relativistic partial wave amplitudes, and may result in a departure of β from the non-relativistic value '2'. Finally, in the autoionization resonance regions [9,10], selective excitations of one relativistic transition amplitude over the other also causes β to depart from '2'.

We first illustrate the methodology by reviewing our recent work on the autoionization resonances in Kr angular distribution asymmetry parameter β [11,12]. The resonances have been identified successfully by controlling in our computational strategy the extent of final state correlations.

In the *4s* photoionization of atomic krypton, autoionization resonances occur below the *3d* ionization thresholds as a result of interchannel coupling between the two

ionization channels ($4s \rightarrow \epsilon p_{3/2}$ and $4s \quad \epsilon p_{1/2}$) from the $4s$ subshell and the six excitation channels ($3d_{5/2} \rightarrow nf_{7/2}$, $3d_{5/2} \rightarrow nf_{5/2}$, $3d_{5/2} \rightarrow np_{3/2}$, $3d_{3/2} \rightarrow nf_{5/2}$, $3d_{3/2} \rightarrow np_{3/2}$ and $3d_{3/2} \rightarrow np_{1/2}$) from the $3d$ subshells. For preliminary investigation of the autoionization region, the RRPA technique was used. It is difficult to identify all the six series of resonances from $3d$ subshells in the same run. Therefore, to characterize the resonances RRPA was employed at three different levels of truncations :

(i) 5 channel calculations :

$4s \rightarrow p_{3/2}, p_{1/2},$

$3d_{5/2} \rightarrow f_{7/2}, f_{5/2}, p_{3/2},$

(ii) 5 channel calculations :

$4s \rightarrow p_{3/2}, p_{1/2},$

$3d_{3/2} \rightarrow f_{5/2}, p_{3/2}, p_{1/2},$

(iii) 20 channel calculations :

$5p_{3/2} \rightarrow d_{3/2}, d_{1/2}, s,$

$5p_{1/2} \rightarrow d_{3/2}, s,$

$4s \rightarrow p_{3/2}, p_{1/2},$

$3d_{5/2} \rightarrow f_{7/2}, f_{5/2}, p_{3/2},$

$3d_{3/2} \rightarrow f_{5/2}, p_{3/2}, p_{1/2},$

$3p_{3/2} \rightarrow d_{5/2}, d_{3/2}, s,$

$3p_{1/2} \rightarrow d_{3/2}, s,$ and

$3s \rightarrow p_{3/2}, p_{1/2}.$

While the set (i) and set (ii) enabled isolating specific correlations, the set (iii) enabled extensive inclusion of most of the RPA correlations that have been included in the present study.

In the present work, experimental thresholds have been used instead of Dirac-Fock (D.F.) thresholds. Certain many-body correlations that are left out in the RRPA can be well accounted using experimental thresholds [14,15]. The experimental thresholds, along with the corresponding Dirac-Fock thresholds, are presented in Table 1.

Figure 1 shows the truncated RRPA results obtained using selective interchannel coupling given in (i) and (ii). At level (i) of truncation, excitation channels only from $3d_{5/2}$ are included in the calculations whereas at level (ii), excitations only from $3d_{3/2}$ are included. From the information obtained from level (i) and (ii) resonance structures are characterized. Finally, using truncation level (iii), the resonances are labeled and compared with the experimental results as shown in Figure 2. The RRPA curve is broken in regions close to the resonances since in these energy regions, the RMQDT technique is better suited and the results are presented separately.

Table 1. Experimental and D F thresholds in eV

Shell	Kr	
	Expt	D.F
$4p_{3/2}$	14 0	14 0
$4p_{1/2}$	14 7	14.74
$4s$	27 5	32.32
$3d_{5/2}$	94 2	101 41
$3d_{3/2}$	95 4	102 79
$3p_{3/2}$	214 8	226.20
$3p_{1/2}$	222 4	234 56
$3s$	293 1	305 43

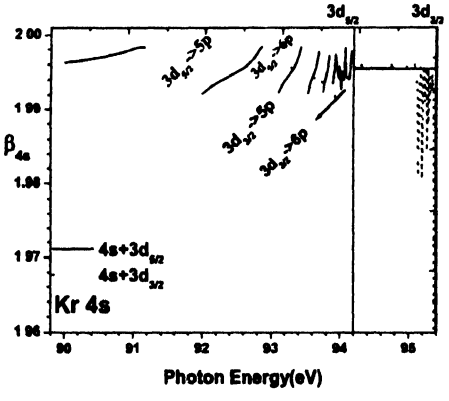

Figure 1. Kr 4s photoionization cross-section at two levels of truncations (i) $4s + 3d_{5/2}$ (solid), (ii) $4s + 3d_{3/2}$ (dotted)

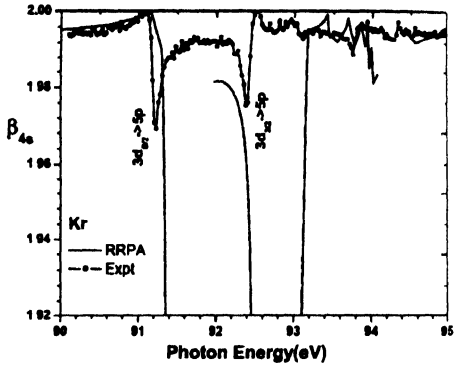

Figure 2. Comparison between theoretical Kr $4s$ β values and experimental values

As can be seen from this Figure, *The positions of resonances show excellent agreement with experiment which is evident from the positions of* $3d_{5/2} \rightarrow 5p$ *and* $3d_{3/2} \rightarrow 5p$ resonances. This is further confirmed in the next section using RMQDT. The calculations clearly indicate deviations of β from 2.0, in qualitative agreement with experiment.

Notice that the RRPA calculations overestimate width of these resonances and also overestimate the deviation of β from 2.0. This can be attributed to the omission of ionization-plus-excitation channels (photoionization satellites) in the calculations. In the next section a detailed study of the autoionization resonances is carried out using RMQDT in conjunction with RRPA.

It may be added that when the channels included at different levels of truncation are all put together, as at level (iii) of truncations certainly the many-body correlation will get affected, but only marginally so.

For the RMQDT analysis, first a few energy points were selected near the $3d_{5/2}$ threshold to extract the *ab initio* RMQDT parameters. Again the methodology of 'selective coupling' of channels to identify the resonances has been used and RRPA + RMQDT has been employed at the following three levels of truncation :

(i) 5ch: channels from $4s$ and $3d_{5/2}$ are coupled,

(ii) 5ch: channels from 4s and $3d_{3/2}$ are coupled,

(iii) 8ch: channels from $4s$, $3d_{5/2}$ and $3d_{3/2}$ are coupled.

The quantum defect parameters have been obtained for each case (not shown) and used for interpolation in the autoionization region. In Figures 3–5 is shown the angular distribution asymmetry parameter β obtained using RMQDT. In the same figures

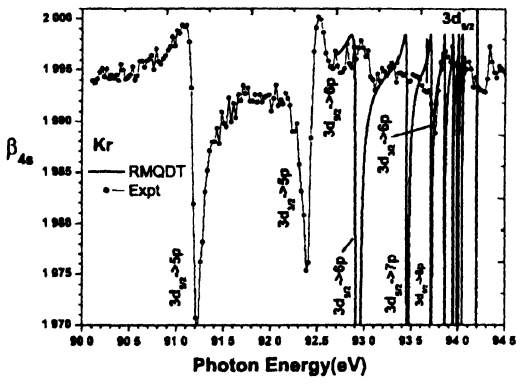

Figure 3. Kr $4s$ β in the truncated RRPA + RMQDT, coupling two ionization channels from $4s$ and three excitation channels from $3d_{5/2}$ along with the experimental results.

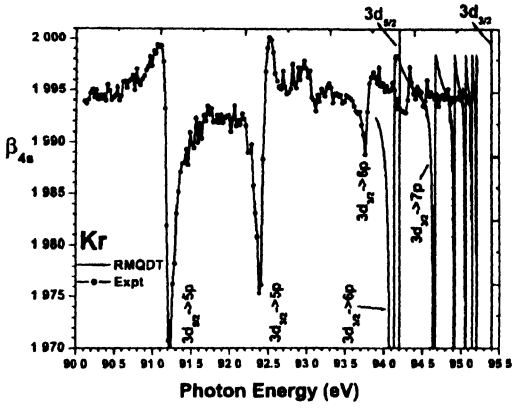

Figure 4. Kr $4s$ β in the truncated RRPA + RMQDT, coupling two ionization channels from $4s$ and three excitation channels from $3d_{3/2}$ along with the experimental results

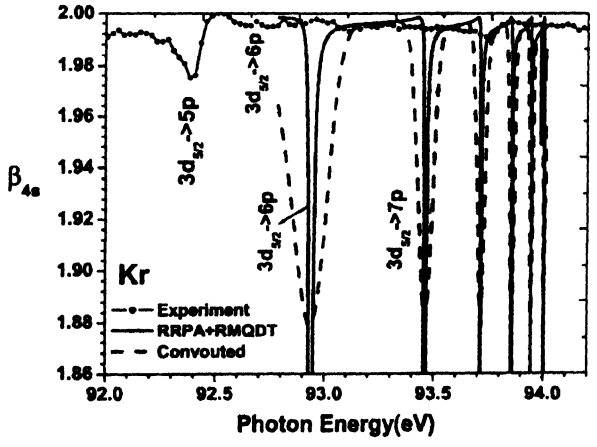

Figure 5. Kr $4s$ β in the truncated RRPA+RMQDT, coupling two ionization channels from $4s$ and six excitation channels fro $3d_{5/2}$ and $3d_{3/2}$ together along with the experimental data. Dashed curve is the convoluted β with a Gaussian of FWHM = 0.50 eV.

are also shown the experimental results obtained by our collaborators [12].

In Figure 5 are presented the results for the angular distribution asymmetry parameter β obtained using level (iii). The resonances shown are the $3d_{5/2}$ excitations to members of the Rydberg series with $n \geq 6$ since the RMQDT parameter vary somewhat for the lowest resonances making the RMQDT method inapplicable [13]. There is a good agreement with respect to position of the resonances obtained from RRPA + RMQDT with the experimental results. This methodology illustrates the success of the computational strategy adopted to characterize complex autoionization spectrum.

There is a strong deviation of β from 2.0 in the resonance region. Akin to the RRPA calculations, the deviation of β from 2.0 is significantly greater than what is observed. This problem can be alleviated, at least partially, by convoluting the calculated β profiles with Gaussian of FWHM 50 meV which corresponds to the experimental resolution. The result is shown as dashed curve. This, however, does not bring theory into complete quantitative agreement with experiment. Overestimation of the deviation of β from 2 is attributed to correlations that are left out in the theoretical formalism. Strong correlation effects (interchannel coupling) causes pronounced variation in the relativistic channels in the region of autoionization resonances making $\beta \neq 2$.

In the next section is discussed the autoionization resonance region below the 5*d* ionization threshold of atomic mercury.

2. Photoionization for 6*s* subshell of atomic mercury below 5*d* ionization thresholds

Selective interchannel coupling was employed to identify the 6*s* autoionization spectrum of Hg. Preliminary studies using RRPA were carried out using four different levels of truncation :

(i) 2 ch: channels only from 6*s* are coupled (intra-shell correlation),

(ii) 5 ch: two channels from 6*s* and three channels from $5d_{5/2}$ are coupled,

(iii) 5 ch: two channels from 6*s* and three channels from $5d_{3/2}$ are coupled and

(iv) 8 ch: two channels from 6*s*, three channels from $5d_{3/2}$ and three channels from $5d_{3/2}$ are coupled.

The analysis of the resonances was thus carried out separately to identify the resonances and then a detailed study was carried out using RMQDT.

In Figure 6 and Figure 7 are shown the RMQDT results obtained from the 5 channel calculations. The 6*s* angular distribution asymmetry parameter was obtained as a function of photon energy, and of the effective quantum number n^*. The resonance structures are periodic, as a function of n^*. In Figures 6 and 7 are also shown the results obtained from the RRPA alone, that is without using the RMQDT. It can be

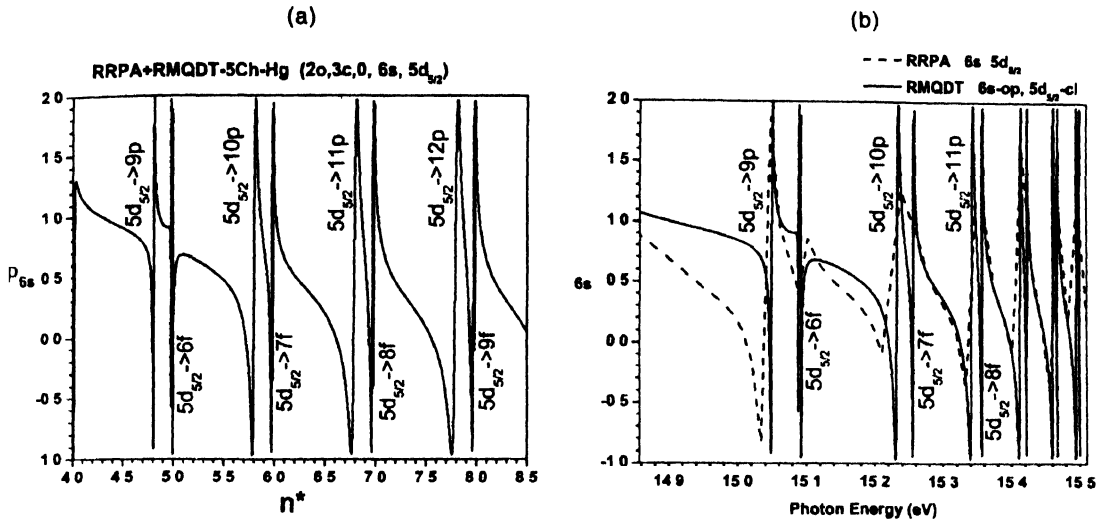

Figure 6. (a) Hg 6*s* angular distribution asymmetry parameter β as a function of effective principal quantum number n^* from RMQDT + RRPA coupling two ionization channels from 6*s* ($6s \rightarrow \epsilon p_{3/2}$ and $6s \rightarrow \epsilon p_{1/2}$) and three excitation channels from $5d_{5/2}$ ($5d_{5/2} \rightarrow nf_{7/2}$, $5d_{5/2} \rightarrow nf_{5/2}$, and $5d_{5/2} \rightarrow np_{3/2}$ (b) Continuous line corresponds to Hg 6*s* β as a function of photon energy from RMQDT + RRPA coupling two ionization channels from 6*s* and three excitation channels from $5d_{5/2}$ as in (a), and dashed line β from RRPA coupling five photoionization channels from 6*s* and $5d_{5/2}$ subshells

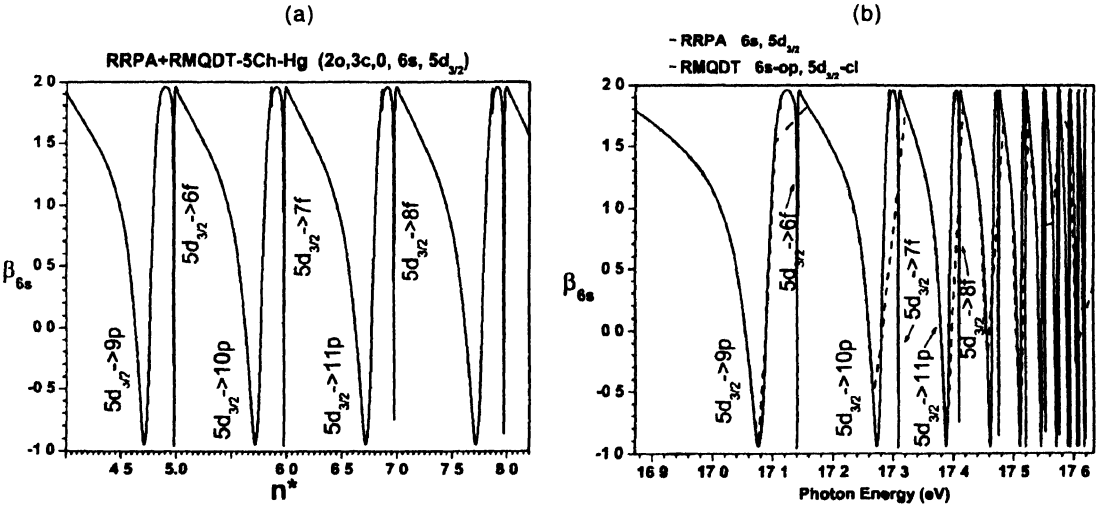

Figure 7. (a) Hg 6*s* angular distribution asymmetry parameter β as a function of effective principal quantum number n^* from RMQDT + RRPA coupling two photoionization channels from 6*s* ($6s \rightarrow \epsilon p_{3/2}$ and $6s \rightarrow \epsilon p_{1/2}$) and three excitation channels from $5d_{3/2}$ ($5d_{3/2} \rightarrow nf_{5/2}$, $5d_{3/2} \rightarrow np_{3/2}$, and $5d_{3/2} \rightarrow np_{1/2}$ (b) Continuous line corresponds to Hg 6*s* β as a function of photon energy from RMQDT + RRPA coupling two ionization channels from 6*s* and three excitation channels from $5d_{3/2}$ as in (a) and dashed line corresponds to β from RRPA coupling five photoionization channels from 6*s* and $5d_{3/2}$ subshells

seen that the resonance positions are identified well in the RRPA calculations The quantum defect values are presented in Table 2. Also presented in the same Table are

Table 2. Quantam defects μ_p and μ_f for atomic mercury.

	RMQDT (present)	HS [16]
μ_p	4.22	4.01
μ_f	1.03	1.02

the quantum defects from an earlier study, using the Hartree-Slater (HS) approximation [16]. As seen from this table, the present results and the HS results [16] show a reasonably good agreement.

The main focus in the present work is on the deviation of $6s$ β from its non-relativistic value $\beta = 2$. At energies of the autoionization resonances, β deviates from '2'. In the case of autoionization resonances seen in the photoionization of the $4s$ subshell of atomic krypton, reported in Section 1, the background value of β was close to ~2. In the case of the $6s$ photoionization of atomic mercury however, β for $6s$ photoionization in the region of $5d$ excitations deviates significantly from '2' *even* in the background region, not merely at resonances. This dramatic deviation of β in the background (non-resonant) energy region is due to the RRPA Cooper minimum in the $6s$ photoionization channels. The deviation of $\beta = 2$ in this energy region is therefore a cumulative effect of the Cooper minimum in $6s$ photoionization, and the resonant excitations from $5d$ subshells.

3. Conclusion

The present work demonstrates the success of employing selective interchannel coupling as a computational strategy to extract detailed physical information in complex atomic spectra. The RRPA + RMQDT method is especially well adapted to use this technique.

4. Acknowledgment

This work was partially supported by Board of Research in Nuclear Sciences (BRNS), Department of Atomic Energy (DAE) and Department of Science and Technology (DST).

References

[1] U Fano *Phys. Rev.* **124** 1866 (1961)

[2] J Bokor, R R Freeman and W E Cooke *Phys. Rev. Lett.* **48** 1242 (1982)

[3] W R Johnson and C D Lin *Phys. Rev.* **A20** 964 (1979)

[4] D L Lin *Phys. Rev.* **A16** 600 (1977)

[5] C M Lee and W R Johnson *Phys. Rev.* **A22** 979 (1980)

[6] J Tulkki *Phys. Rev. Lett.* **62** 2817 (1989)

[7] O Hemmers, S T Manson, M M Sant'Anna, P Focke, H Wang, I A Sellin and D W Lindle *Phys. Rev.* **A64** 022507 (2001)

[8] Z Altun and S T Manson *Phys. Rev.* **A61** 030702 (2000)

[9] D Dill *Phys. Rev.* **A7** 1976 (1973)

[10] S B Whitfield, B D Krosschell and R Wehlitz *J. Phys.* **B37** 3435 (2004)

[11] S B Whitfield, R Wehlitz, H R Varma, T Banerjee, P C Deshmukh and S T Manson *J. Phys.* **B39** L335 (2006)

[12] Hari R Varma *PhD Thesis* (Submitted to Indian Institute of Technology Madras, India) (2007)

[13] P C Deshmukh and S T Manson *Phys. Rev.* **A28** 209 (1983)

[14] W R Johnson, V Radojević, Pranawa Deshmukh and K T Cheng *Phys. Rev.* **A25** 337 (1982)

[15] Steven L Carter and Hugh P Kelly *J. Phys.* **B11** 2467(1978)

[16] S T Manson *Phys. Rev.* **182** 97 (1969)